

## Photocatalysis

International Edition: DOI: 10.1002/anie.201702213  
German Edition: DOI: 10.1002/ange.201702213

## Synthesis of Layered Carbonitrides from Biotic Molecules for Photoredox Transformations

Can Yang, Bo Wang, Linzhu Zhang, Ling Yin, and Xinchen Wang\*

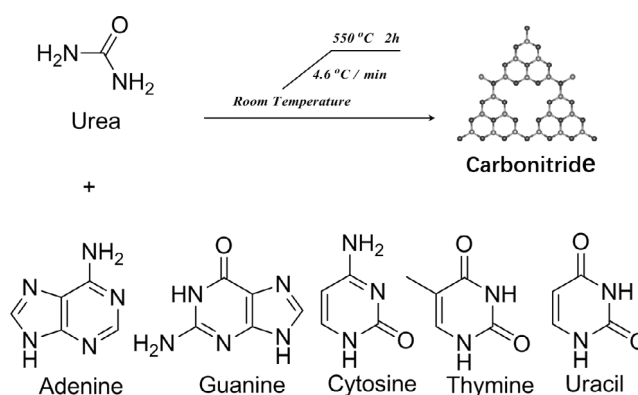
**Abstract:** The construction of layered covalent carbon nitride polymers based on tri-*s*-triazine units has been achieved by using nucleobases (adenine, guanine, cytosine, thymine and uracil) and urea to establish a two-dimensional semiconducting structure that allows band-gap engineering applications. This biomolecule-derived binary carbon nitride polymer enables the generation of energized charge carrier with light-irradiation to induce photoredox reactions for stable hydrogen production and heterogeneous organosynthesis of C–O, C–C, C–N and N–N bonds, which may enrich discussion on chemical reactions in prebiotic conditions by taking account of the photoredox function of conjugated carbonitride semiconductors that have long been considered to be stable HCN-derived organic macromolecules in space.

Conjugated polymers both in their neutral and charged states have gained great attention due to their promising applications in electronic devices, such as light-emitting diodes, lasers, photovoltaic cells, field-effect transistors, and biology.<sup>[1–6]</sup> More recently, the applications have experienced an extension to photoredox catalysis by acting as flexible light transducers to enable the construction of soft photosynthetic machinery/device by using easy solution and thermal processes.<sup>[7–10]</sup> Current interest in the emerging field of organic photocatalysis has focused on the molecular design and modification of conjugated semiconductors, such as graphitic carbon nitrides (g-CN) and covalent organic frameworks with spatially extended  $\pi$ -bonding systems.<sup>[11–13]</sup> Being a stable photocatalyst with a two-dimensional conjugated structure and reduced exciton-binding energy,<sup>[14]</sup> g-CN has shown great promise for water splitting,<sup>[15]</sup> CO<sub>2</sub> reduction,<sup>[16]</sup> and organosynthesis,<sup>[17,18]</sup> which has triggered much research devoted to organic photocatalysis for energy and environmental applications.

Many synthetic strategies, including molten-salt growth<sup>[19–21]</sup> templating<sup>[22]</sup> and (solvo)thermal condensation<sup>[23]</sup> syntheses, have been applied to obtain g-CN nanostructures with high performance. In particular, thermal condensation is a facile and widely adopted approach to drive the construction and connection of triazine and heptazine tectons to polyconjugated systems, mostly using nitrogen-containing com-

pounds such as cyanamide, dicyanamide, triazine and heptazine derivatives. Further modifications on the chemical and physical properties by doping and extending its electron delocalization were achieved by using aromatic precursors containing heteroatoms, including B, S, N and P. For example, efficient g-CN photocatalysts have been prepared by the polymerization of dicyandiamide with 2-aminobenzonitrile or 2,4-diaminoquinazoline,<sup>[12]</sup> and the condensation of urea with barbituric acid, 2-aminothiophene-3-carbonitrile or diaminomaleonitrile.<sup>[14]</sup> Considering the diverse array of organic precursors with different chemical compositions and electronic structures, it practically allows the one-pot design of polymer photocatalysts on a molecular level in a rational manner, but also enables band-gap engineering, donor/acceptor design, topological fabrication and modifications of their physical properties such as p/n characteristics.<sup>[24]</sup>

In contrast to ordinary organic precursors, here we move one step forward by applying biotic compounds to construct g-CN semiconductors using nucleobases and urea, to answer the question if g-CN can be produced from life's molecules (Scheme 1).<sup>[25]</sup> All these compounds are existent in biotic



**Scheme 1.** The chemical production of polymeric carbon nitride semiconductors from nucleobases and urea.

conditions as life's building blocks from simple precursors in the primordial soup.<sup>[26,27]</sup> We are therefore interested and encouraged to enrich the studies on prebiotic (photo)chemistry, where HCN polymeric clusters (including triazine-based super carbonitride tectons) have been considered as the most readily formed and most stable organic macromolecules in space.<sup>[28]</sup> The utilization of these biological precursors for the chemical synthesis of g-CN-based semiconductors by thermally induced condensation is representative of the extreme terrestrial and thalassic thermal/hydrothermal conditions of primordial Earth; for example the temperatures in hydro-

[\*] C. Yang, B. Wang, L. Zhang, L. Yin, Prof. X. Wang  
State Key Laboratory of Photocatalysis on Energy and Environment,  
College of Chemistry, Fuzhou University  
Fuzhou 350002 (China)  
E-mail: xcwang@fzu.edu.cn  
Homepage: <http://wanglab.fzu.edu.cn>

Supporting information for this article can be found under <https://doi.org/10.1002/anie.201702213>.

thermal vents close to the volcanic edifices have been found to range from about 60 °C to 500 °C. The potential existence of photoactive g-CN semiconductors in primordial environments to induce photoredox transformations of water, CO<sub>2</sub> and organics would enrich the discussion on the chemical evolution of life. Furthermore, the study is also of relevance for the artificial photosynthesis field.

Nucleobases [adenine (A), guanine (G), cytosine (C), thymine (T) and uracil (U)] are readily available and stable precursors. Surprisingly, according to our knowledge, there is no report on the synthesis of carbon nitride from biomass-derived building blocks. Here, we propose a facile synthesis of carbon nitride based materials by thermal condensation of 1) urea with 2) A, G, C, T and U, respectively. We aim to demonstrate that the incorporation of such building blocks can lead to the development of carbon nitride for H<sub>2</sub> production, and potentially to induce photoredox transformations under prebiotic conditions.

In a typical synthesis, a certain amount of nucleobase (0, 5, 15, 30, 50, 80 mg) and urea (10 g) were dissolved in water with stirring, followed by heating at 80 °C to evaporate water. Afterwards, the obtained mixture was calcined at 400–550 °C in air. The obtained samples are denoted as CNX, where X represents the nucleobase. The reference sample from urea is denoted as g-CN.

The chemical structure and composition of CNX samples were characterized by X-ray diffraction (XRD) (Figure S2a in the Supporting Information) and Fourier transform infrared spectroscopy (FT-IR) (Figures S2b and S3). The XRD patterns of the samples in Figure S2a show a strong peak at 27.4° related to the (002) interlayer reflection of a layered crystal, plus a weak reflection at 13° due to the in-plane repeating unit of heptazine. The FT-IR spectrum in Figure S2b features distinct peaks from 1200 to 1600 cm<sup>-1</sup> corresponding to the stretch modes of aromatic CN heterocycles, while the breathing mode of the triazine units corresponds to 810 cm<sup>-1</sup>. The broad peaks between 3500 and 3100 cm<sup>-1</sup> originate from N–H stretches on the surface of the carbon nitride due to the surface defective sites as a result of incomplete condensation. These results clearly confirmed that all of the CNX materials are featuring similar crystal and chemical structure of graphitic carbon nitride.

Then, we investigated the photocatalytic activities of CNX samples in water splitting and revealed the effect of different nucleobase monomers on the photocatalytic performances. As shown in Figure S4, the hydrogen evolution rates (HER) of CNX materials increase by 6–8 times as compared

to urea-derived g-CN under visible light irradiation. Moreover, the photocatalyst synthesized from urea with cytosine (CNC) exhibits the best activity for producing hydrogen among all these samples. The superior photocatalytic performance of CNC is probably due to the better interaction and structural matching between cytosine and urea. Since one cytosine molecule could break into two molecules with the similar structure to urea under thermal treatment, the chemical structure of cytosine enables closer combination with urea and better conjugation into the covalent carbon nitride frameworks. On the contrary, the polymerization of urea with other nucleobases with more functional groups is less straightforward due to steric hindrance. Therefore, cytosine, which could polymerize with the urea best, was selected as the monomer to synthesize modified carbon nitride polymers with high efficiency for photocatalytic reactions.

A series of photocatalysts were prepared from mixtures of urea and different amounts of cytosine. These materials are denoted as CNC<sub>y</sub>, where y stands for the amount of cytosine (y mg). As shown in Figure 1b and Figure S3 the XRD pattern and FT-IR spectrum of CNC<sub>y</sub>, respectively, are very similar to those of urea-derived g-CN, which demonstrates that the graphitic carbon nitride based structure is maintained with increasing amount of cytosine. The surface morphology and texture of the CNC<sub>30</sub> sample (after Pt deposition) were investigated by scanning electron microscopy (SEM) and transmission electron microscopy (TEM) (Figure 1a). In the TEM image smooth, flat layers can be seen, and the Pt particles were distributed uniformly on the surface after reaction (Figure 1a). There was no obvious difference

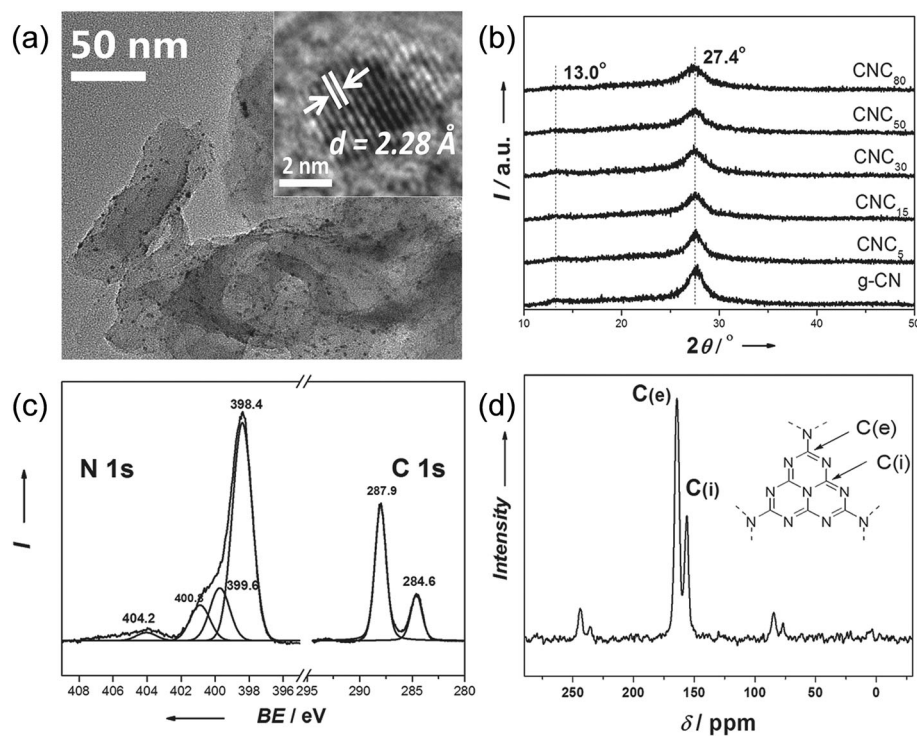


**Figure 1.** a) TEM of Pt@CNC<sub>30</sub> after reaction. Inset: HR-TEM of Pt nanoparticles. b) XRD patterns of different CNC samples. c) XPS analysis of CNC<sub>30</sub> sample. d) Solid-state <sup>13</sup>C NMR spectrum of CNC<sub>30</sub>.

between the morphologies of the sample before and after reaction. During the process of photo-reduction, the Pt nanoparticles were dispersed on the surface of g-C<sub>3</sub>N<sub>4</sub>, and the size distribution of Pt NPs ranged from 3 to 5 nm (Figure 1a, inset), the lattice distance of Pt NPs is 2.28 Å.

The solid-state <sup>13</sup>C NMR spectra of CNC<sub>30</sub> (Figure 1d) shows two peaks, the first peak at 164.3 ppm is ascribed to the C(e) atoms [CN<sub>2</sub>-(NH<sub>2</sub>)], whereas the second one at 155.6 ppm is attributed to the C(i) atoms of melem (CN<sub>3</sub>). These signals confirm the existence of poly(tri-s-triazine) structure in CNC<sub>30</sub>. In the XPS survey spectrum (Figure 1c and S5b–d), there are three elements (C, N and O), similar to those of g-CN. The O1s peak present in CNC<sub>30</sub> is due to the surface-absorbed H<sub>2</sub>O or CO<sub>2</sub>, as cross-checked by the FT-IR analysis (Figure 1).

By increasing the resolution of XPS analysis, we observed two main carbon species in the C1s spectrum (Figure S5). One carbon species with a binding energy (BE) of 287.9 eV is identified as sp<sup>2</sup>-bound carbon (C=C=C), the other with BE of 284.6 eV was due to carbon impurities. The N1s XPS spectrum can be deconvoluted into four peaks at 398.4, 399.6, 400.8, and 404.2 eV. The strongest N1s peak at 398.4 eV was assigned to sp<sup>2</sup>-bound N in N-containing aromatic rings (C=N=C), whereas the weak peak at 399.6 eV is attributed to the tertiary nitrogen N-(C)<sub>3</sub> groups. The peak at 400.7 eV indicated the presence of amino groups (C-N-H) and the peak at 404.2 eV was attributed to charging effects or positive charge localization in heterocycles.

Figure 2a displays the UV/Vis diffuse reflectance spectra (DRS) of the sample. The optical absorption is red-shifted from 460 nm for g-CN to 470 nm for CNC<sub>30</sub> and finally to 480 nm for CNC<sub>80</sub>, corresponding to the change of sample color from pale yellow to deep yellow and to orange. These changes are attributed to the combination of cytosine monomer in the CN that effectively broadens the conjugated π-electron system and thus narrows the semiconductor band gap, which is also reflected by PL analysis (Figure 2b) showing gradually red-shift of the emission peaks with increasing amount of cytosine added. The effect of cytosine addition on the band structure (valence band and conduction band level) is shown in Figure S6.

With gradual integration of cytosine into the CN network, electron paramagnetic resonance (EPR) intensity increases progressively, due to a well-evolved electronic structure with extended delocalization of the π-conjugated system (Figure S7). As expected, the generation of photochemical radical pairs can be efficiently promoted by this extended π-

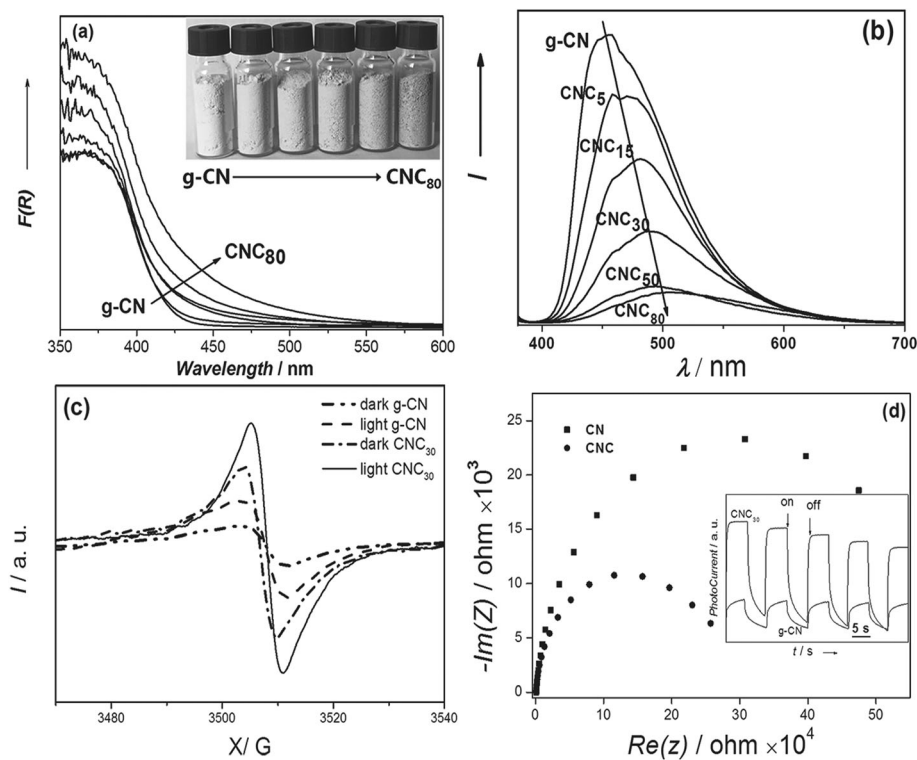


**Figure 2.** a) UV/Vis DRS spectra. Inset: photograph of the samples. b) Photoluminescence spectra under 400 nm excitation. c) EPR spectra of CNC<sub>30</sub> in the dark (dashed) or with visible light (solid), g-CN as a reference. d) EIS Nyquist plots. Inset: photocurrent of g-CN and CNC<sub>30</sub>, on/off photocurrent response at  $-0.2$  V bias potential vs. Ag/AgCl in  $0.2$  M Na<sub>2</sub>SO<sub>4</sub> solution.

conjugated system (see Figure 2c dashed dot line), thus resulting in an enhanced EPR signal in dark condition. When the samples were irradiated with visible light, the signal could be enhanced further (Figure 2c, solid lines).

The (photo)electrochemical properties of the CNC<sub>30</sub> sample was examined by electrochemical impedance spectroscopy (EIS) and photocurrent test. A marked decrease of Nyquist plots diameter for CNC<sub>30</sub> is observed in Figure 2d, which demonstrated that the electronic resistance of CNC<sub>30</sub> is smaller compared to pristine g-CN. At the same time, the photocurrent of CNC<sub>30</sub> increased by a factor of four compared to g-CN (Figure 2d inset). This photocurrent enhancement illustrates that the mobility of the photo-excited charge carriers is promoted.

The samples were evaluated in a photocatalytic hydrogen evolution assay by loading 3 wt.% Pt as co-catalyst and using triethanolamine (TEOA) as a hole scavenger. Figure 3a shows that all CNC samples exhibit better catalytic activity in hydrogen evolution than the pure g-CN. Notably, the CNC<sub>30</sub> sample shows the highest activity for hydrogen production. With increasing amount (from 5 mg to 30 mg) of cytosine in the CNC samples, HER becomes gradually faster. The activity decreased when further increasing the amount of cytosine to 80 mg ( $60 \mu\text{mol h}^{-1}$ ), but is still higher than with pure g-CN ( $37 \mu\text{mol h}^{-1}$ ). With 30 mg cytosin an optimum HER ( $282 \mu\text{mol h}^{-1}$ ) is achieved, which is nearly 8 times faster than with pure g-CN.

The photocatalytic performance of CNC<sub>30</sub> is well consistent with its optical absorption (Figure 3b), and the amount of

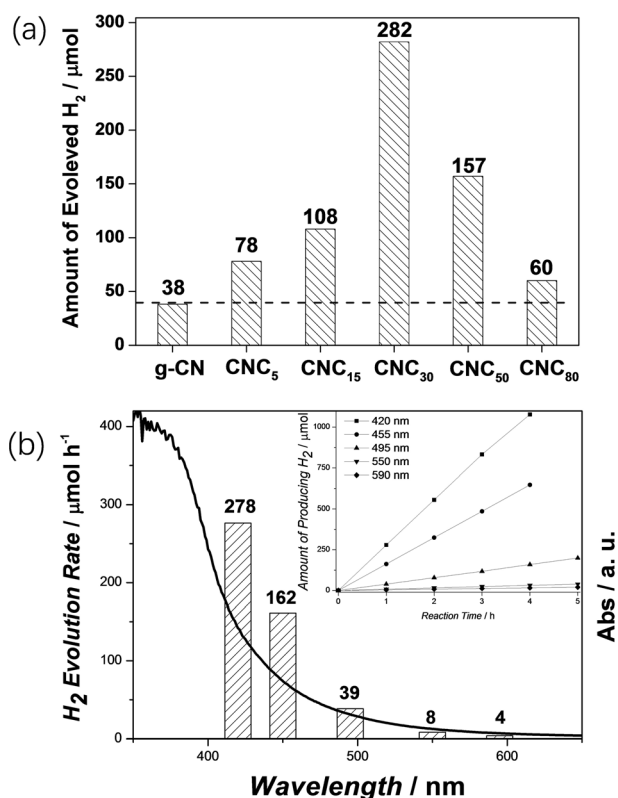


**Figure 3.** Photocatalytic hydrogen evolution activity of the samples. a) The effect of cytosine amount on HER. b) Wavelength dependence of the HER with CNC<sub>30</sub> loaded with 3 wt.% Pt. Inset: time-dependence of the HER with CNC<sub>30</sub> at different irradiation wavelengths.

H<sub>2</sub> increased linearly with time under different wavelengths (Figure 3b, inset), suggesting that the main driving force of the photocatalytic reaction is the harvested visible photons.

The stability of CNC<sub>30</sub> was examined by operating the experiments under the same reaction conditions for several runs (Figure S8). Except for the first run, the reaction was treated without light for one hour to ensure there was no H<sub>2</sub> gas in the reaction system. A slight deactivation was noticed in the first four runs. When an appropriate amount of TEOA was added to the reaction solution, the activity of H<sub>2</sub> evolution improved in the fifth run. This indicates that the decrease in activity after the first run is mainly due to the decreased concentration of TEOA. It is noted that no obvious structural changes were observed (Figure S9–S10).

Next, the apparent quantum yield (AQY) of the best sample was examined by studying catalytic kinetics using different amount of photocatalysts. Figure S11 shows that AQY initially increases with increasing amounts of CNC<sub>30</sub>, then reaches a plateau at a maximum value of 7.1% before decreasing slightly upon further increasing the amount of catalyst. We therefore applied 75–100 mg sample to check the intrinsic AQY where the reaction is limited by charge separation at the interface to rule out mass diffusion effects.

We further studied the photocatalytic activity of CNC<sub>30</sub> in CO<sub>2</sub> reduction (Figure S12–S13), using Co(bpy)<sub>3</sub>Cl<sub>2</sub> as redox mediator and TEOA as electron donor under visible light ( $\lambda > 420$  nm). CNC<sub>30</sub> photocatalyzed the generation of CO

(32.3  $\mu$ mol) and H<sub>2</sub> (8.02  $\mu$ mol), with a selectivity for CO production of 80.1% (entry 1 in Table S1). CNC<sub>30</sub> gives the highest yield and selectivity for CO production, and there is no detectable production of CO in the absence of either CNC<sub>30</sub> or light (entries 2 and 3 in Table S1). The evolution of CO was not observed when CO<sub>2</sub> was replaced with Ar gas (entry 6 in Table S1), which together with the isotopic experiments (Figure S14) confirmed that the source of CO is CO<sub>2</sub> and not organic sources present in the system.

Besides H<sub>2</sub>O and CO<sub>2</sub>, the process of photochemical evolution involves a series of organic reactions. We therefore checked the potential capability of the synthetic g-CN in photocatalyzing the redox transformation of organic molecules, including amines, alcohols and the coupling of C–C, C–O, C–N and N–N bonds (Table 1). As shown in entry 1,

**Table 1:** Different organic reactions driven by the CNC<sub>30</sub> photocatalyst.

Entry	Reaction	Conv. [%]	Sel. [%]
1 <sup>[a]</sup>		79	98
2 <sup>[b]</sup>		19.8	96.5
3 <sup>[c]</sup>		56	94
4 <sup>[d]</sup>		99.3	98
5 <sup>[e]</sup>		61.4	90

Reaction conditions: [a] Substrate (1 mmol), catalyst (50 mg), CH<sub>3</sub>CN (10 mL) as solvent, 80°C, O<sub>2</sub> (1 MPa). [b] Substrate (1 mmol), catalyst (50 mg), CH<sub>3</sub>CN (4 mL) as solvent, 160°C, O<sub>2</sub> (1 MPa), 24 h. [c] Substrate (0.1 mmol), catalyst (5 mg), trifluorotoluene (1.5 mL) as solvent, 60°C, O<sub>2</sub> (1 MPa), 3 h under visible light irradiation. [d] Iodobenzene (0.15 mmol) and benzeneboronic acid (0.6 mmol), catalyst (10 mg with 3 wt.% Pd), 2.5 mL of water and 2.5 mL of ethanol, K<sub>2</sub>CO<sub>3</sub> (1 mmol), 30°C, 2 h under visible light irradiation. [e] 30 Vol.% substrate aqueous solution, catalyst (100 mg), 1 wt.% Pt, 24 h under UV/vis light illumination. All products were detected by GC-MS.

amines can be photooxidized into imines by g-CN under oxygen atmosphere, which are regarded as important electrophilic intermediates in organic synthesis. The conversion is 79% and the selectivity 98%. Activation of sp<sup>3</sup> C–H bonds can also be achieved, for instance, in entry 2, the CH<sub>2</sub> group was oxygenated to C=O selectively. The C–O bond in benzyl alcohol could be oxidized to C=O (entry 3). In addition, as shown in entries 4 and 5, the synthesized g-CN is also an active photocatalyst for the coupling of aromatic halides and the cross-linking of ketone and alcohol. Of particular note, the reactions in entries 4 and 5 are both anaerobic reactions under light-irradiation, suggesting a link to the evolution of algae for photosynthesis. All reactions mentioned above proceed with excellent selectivity and yield, which proves that heterogeneous photocatalysis offers a promising route to realize green organic syntheses under solar irradiation in ambient conditions.

In conclusion, we have demonstrated a biotic precursor approach to manipulate the texture, surface and optical properties of g-CNX polymers synthesized from urea and nucleobases. By optimizing the synthetic recipe, hydrogen evolution reaction under visible light ( $\lambda > 420$  nm) reached



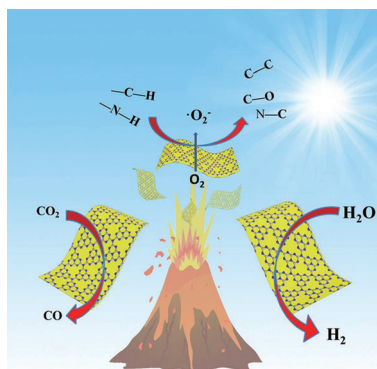
## Communications



## Photocatalysis

C. Yang, B. Wang, L. Zhang, L. Yin,  
X. Wang\* ————— ■■■■-■■■■

Synthesis of Layered Carbonitrides from  
Biotic Molecules for Photoredox  
Transformations



**A prebiotic photocatalyst?** Graphitic carbon nitrides synthesized from nucleobases and urea enable the photogeneration of charge carriers to induce photoredox reactions for  $\text{H}_2$  production and heterogeneous organosynthesis of C–O, C–C, C–N and N–N bonds. The findings enrich the concept of photochemical reactions in the primordial soup.